Multi-slice Myelin Water Imaging for Practical Clinical Applications at 3.0 T

Junyu Guo[1], Qing Ji[1], and Wilburn E. Reddick[1]
[1]*Division of Translational Imaging Research, St Jude Children Research Hospital, Memphis, TN, United States*

INTRODUCTION: Myelin water imaging is a promising, noninvasive technique for evaluating white matter diseases and monitoring myelination in early childhood. Poor image quality and a long acquisition time are major obstacles to practical clinical applications [1]. In this study, a novel postprocessing method with an efficient multi-slice acquisition scheme, called T_2 spectrum analysis using a weighted regularized non-negative least squares algorithm and non-local mean filter (T_2SPARC), is presented to overcome these obstacles and achieve a shorter acquisition time, higher image quality, and large volume coverage. In vivo results from healthy volunteers and a patient with leukoencephalopathy (LE) showed that the T_2SPARC method can generate robust and high-quality myelin water fraction (MWF) maps of 10 slices within 11 minutes.

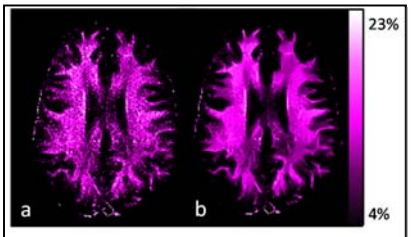

Fig. 1 Effects of non-local mean (NLM) filter. (a) MWF map without the non-local mean filter. (b) Corresponding MWF with the NLM filter.

METHOD: A modified multi-slice CPMG sequence with a refocusing slice thickness three times the size of the excitation slice thickness was used to optimize T2 decay curves [2]. The acquisition scheme includes two scans, each of which acquires five slices and has a slice gap twice as large as the excitation slice thickness [2,3]. The position of the second scan is shifted 7.5 mm along the slice direction relative to the first scan. Imaging data were acquired using a 12-channel head coil on a 3T scanner (Trio, Siemens). The protocol for the scans was as follows: FOV = 220×220 mm; slice thickness = 5 mm; acquisition matrix, 256x256; 5 slices with a 200% slice gap; 32 echoes and TEs = 10·N ms (N = 1,2,3, …, 32); TR = 3000 ms; receiver bandwidth = 300 Hz/pixel; GRAPPA reduction factor = 2, and the number of reference lines = 24. The acquisition time for each scan was about 5 minutes 29 seconds, and the total time for two scans was 11 minutes.

In this study, a weighted regularized nonnegative least squares (wrNNLS) algorithm was used to minimize the residue norm and smooth the T2 distribution density curve [2]. The wrNNLS algorithm is as follows:

$$\min_{S_T}\{\left\|ES_T - Y\right\|_2 + \mu\left\|WS_T\right\|_2\},\ E_{nm} = e^{-\frac{t_n}{T_{2m}}}, W_m = 1/\Delta T_{2m},\ S_T \geq 0 \qquad (1)$$

where S_T is the weighted spectral amplitude, Y is the decay signal intensity, t_n is the n^{th} echo time, ΔT_{2m} is a logarithmic T_2 interval, and μ is the regularization coefficient. The number of T_2 sampling points of 96 was chosen to balance computation efficiency and spectral accuracy. An empirically optimized value of μ = 1.8 was used for regularization to balance the sensitivity and reliability to measure MWF values for different or similar types of brain tissue.

The T_2 spectrum can be partitioned into four intervals: myelin water, T_2=15–40 ms; intra- and extracellular water, 40–200 ms; tissue water with long T_2, 200–800 ms; and cerebral spinal fluid, 800–2000 ms. For each pixel, the ratios of the direct summation of S_T within each interval to its overall summation corresponding to MWF, intra- and extracellular water fraction (IEWF), long T2 water fraction (LWF), and cerebral spinal fluid fraction (CSFF) were computed to generate parametric maps. Even though the sensitivity to noise can be dramatically diminished by using wrNNLS with μ = 1.8, parametric maps of MWF still appear noisy compared to conventional clinical images. An NLM filter can be used to further denoise those parametric maps and improve their SNRs [4]. Two healthy volunteers and one patient with LE were imaged in the preliminary study.

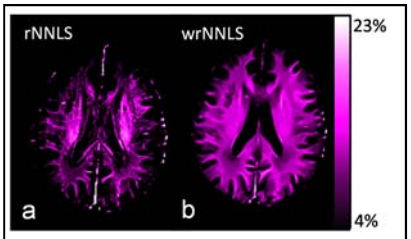

Fig. 2 MWF maps using the rNNLS and wrNNLS algorithms. (a) MWF map using the rNNLS algorithm with μ= 0.26; (b) MWF map using the wrNNLS algorithm with μ= 1.8.

RESULTS: The effect of the NLM filter is shown in Fig. 1. Fig. 1a shows the original MWF map without using the NLM filter, and Fig 1b shows the filtered MWF map, which is dramatically improved over the original map without blurring. So the NLM filter played a larger role in the final MWF map when noise was the primary issue in data postprocessing. Two MWF parametric maps using the regularized nonnegative least squares (rNNLS) and wrNNLS algorithm were compared and shown in Fig.2. MWF using rNNLS and μ=0.26 [5] is shown in Fig.2a. MWF using wrNNLS and μ=1.8 is shown in Fig. 2b. There was an impressive difference between the two algorithms. The MWF was dramatically underestimated in the edge region of the brain using rNNLS in comparison with wrNNLS. The MWF values were 6.3% for rNNLS and 11.4% for wrNNLS in the forceps minor. The quality of the parametric maps using wrNNLS was dramatically improved over those using rNNLS. Fig. 3 shows parametric maps from the T_2SPARC method for a healthy volunteer and a patient with LE in a similar slice position. Three elliptical ROIs were drawn in the volunteer's and the patient's T_2-weighted (T_2w) image. For the patient, the red ROI was in normal white matter; the green and yellow ROIs were in lesions; the green and yellow arrows point to lesions in the parametric maps. Normal MWF values in red ROIs from the volunteer and the patient were similar (12.3% and 11.1%, respectively). MWF values from the green and yellow lesion ROIs were 1.9% and 4.5% in the patient, which were substantially lower than the MWF values from similar regions in the volunteer (11.0% and 12.3%). The LWF in the green ROI from the patient was 8.3%, which was dramatically beyond the normal value (0%).

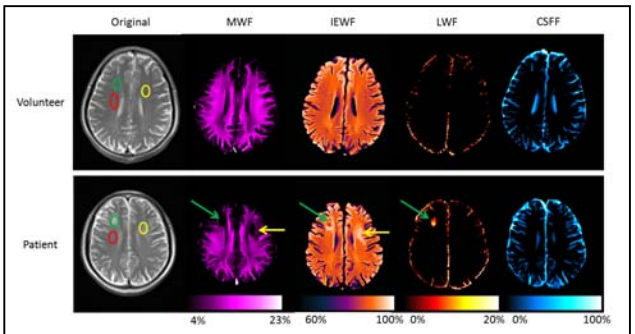

Fig. 3 Comparison of parametric maps between a healthy volunteer and a patient with LE. T_2w image and four parametric maps from a healthy volunteer are in the first row, and the corresponding images of a patient are in the second row.

CONCLUSION: We present the T_2SPARC method, including an efficient acquisition scheme and a robust and new postprocessing technique for generating MWF maps. We have shown remarkable in vivo results from healthy volunteers and one LE patient. This method allowed a shorter acquisition time and provided higher image quality and large volume coverage for practical clinical applications. Furthermore, this method yields additional parametric maps such as IEWF, LWF, and CSFF, which can also be useful as a noninvasive means to identify lesions in different brain diseases.

REFERENCE:

1. Whittall et al. MRM, 1997. 37(1): p. 34-43.
2. Guo et al. ISMRM, 2011, 4481.
3. Guo et al. MRM, 2012, in press.
4. Buades et al, CVPR'05, 2005. 2: p. 60-65.
5. Ji et al. ISMRM, 2011: 4562.